18 Gated Ion Channel-Based Biosensor Device

Frances Separovic and Bruce A. Cornell

18.1 Introduction

A biosensor device based on the ion channel gramicidin A (gA) incorporated into a bilayer membrane is described. This generic immunosensing device utilizes gA coupled to an antibody and assembled in a lipid membrane. The membrane is chemically tethered to a gold electrode, which reports on changes in the ionic conduction of the lipid bilayer. Binding of a target molecule in the bathing solution to the antibody causes the gramicidin channels to switch from predominantly conducting dimers to predominantly nonconducting monomers. Conventional a.c. impedance spectroscopy between the gold and a counter electrode in the bathing solution is used to measure changes in the ionic conductivity of the membrane. This approach permits the quantitative detection of a range of target species, including bacteria, proteins, toxins, DNA sequences, and drug molecules.

18.2 Membrane-Based Biosensors

The use of a synthetic molecular membrane as the basis for a chemical sensor was proposed 40 years ago (Toro-Goyco et al., 1966). The effect of protein–protein interactions between a bilayer lipid membrane (BLM) and species in the bathing solution was reported via the admittance of the BLM. However, a major practical issue was the stability of the membrane against mechanical damage. Membranes made from polymerized lipids were considered to be more stable (Ligler et al., 1988) and bacteriorhodopsin, the light sensitive bacterial proton pump, was incorporated into polymerized liposomes and observed to function (Yager, 1988; Zaitsev et al., 1988). A membrane-based biosensor device for the detection of biological toxins (Ligler et al., 1998) also used polymerized lipids, with alamethicin and a calcium channel complex in a BLM supported on a porous silicon substrate. The porous silicon gave mechanical support for the lipid membrane as well as acting as a reservoir for the transmembrane flow of ions. The range of applications of the device was limited by the stability of the receptor–membrane complex: from the inherently labile calcium channel complex and the mechanical instability of the supporting membrane. We have addressed this essential instability by using gA as the ion channel and a tethered membrane on a gold surface as a biosensor device (Cornell et al.,

1997). Once the first lipid monolayer is physisorbed and/or chemically attached to the surface, a second layer of mobile lipids is fused onto the tethered monolayer to form a tethered BLM (see reviews by Sackman, 1996; Plant, 1999). Receptors are attached to gA in order to gate the ionophore.

18.3 The Ion Channel Switch ICS^{TM} Biosensor

A biosensor based on gA, a low molecular weight bacterial ion channel, has been used for the detection of low molecular weight drugs, proteins, and microorganisms (Cornell et al., 1997; Anastasiadis and Separovic, 2003). Gramicidin A is a 15 residue peptide of alternating L- and D- amino acids and two gA molecules form a monovalent cation channel across the lipid bilayer (Wallace, 1998). The Ion Channel Switch (ICS^{TM}) biosensor (Fig. 18.1) employs a disulfide lipid monolayer tethered to a gold surface by a polar spacer, which provides a reservoir for ions permeating through the membrane. The transduction mechanism depends on the gA properties within a BLM. Gramicidin A monomers diffuse within the individual monolayers of the BLM. The flow of ions through gA occurs when two nonconducting monomers align to form a conducting dimer. In the biosensor, however, the gA molecules

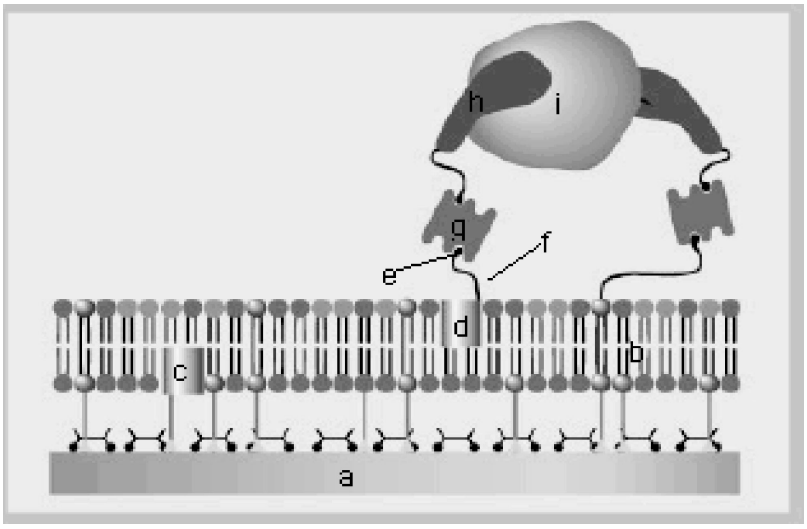

Fig. 18.1 The Ion Channel Switch^{TM} biosensor consisting of a gold electrode (a) with tethered lipid bilayer (b). Embedded in the lipid bilayer are two gA analogues, one fixed (c) and a mobile gA (d) with biotin (e), attached through an aminocaproyl linker (f). Biotin binds strongly to streptavidin (g). When the biotinylated receptor (h) binds to a desired target molecule (i), the mobile gA (d) in the upper monolayer is immobilized and, therefore, is not able to align with the fixed gA (c) in the lower monolayer to form an ion channel. Hence ion current flow to the gold electrode below is decreased when an analyte is detected.

within the tethered inner leaflet of the lipid bilayer are also tethered whilst those on the outer monolayer are free to diffuse and are attached to antibodies. The binding of an analyte cross-link antibodies attached to the membrane spanning lipid tethers to those attached to the mobile outer layer channels. Due to the low density of tethered gA molecules within the inner membrane leaflet, this anchors the cross-linked gA distant, on average, from their immobilized inner layer channel partners. Gramicidin dimer conduction is thus prevented and the admittance of the membrane is decreased. Application of a small alternating potential between the gold substrate and a reference electrode in the test solution generates a charge at the gold surface and causes electrons to flow in an external circuit.

Biological lipid membranes are liquid crystalline and the outer leaflet of the biosensor membrane is effectively a 2D liquid crystal. The antibodies attached to the mobile ion channels are able to scan a significant membrane area in a few minutes and thus have access to multiple antibody sites attached to membrane spanning lipid tethers. Hence, the ICS^{TM} biosensor responds more rapidly than if simply binding to antibodies attached to the mobile gA channels triggered the transduction mechanism. The response speed of the biosensor is improved in direct proportion to the number of binding sites accessible to the mobile channels, analogous to an electronic multiplexer.

Tethering the inner monolayer to the gold surface enhances the stability of the membrane but additional stability is achieved by using "archaebacterial lipids." These are lipids modeled on constituents found in bacteria capable of surviving extremes of temperature and hostile chemical environments. The hydrocarbon chains of these lipids span the entire membrane, (Kushawaha et al., 1981) and ether linkages replace the esters (de Rosa et al., 1983). BLM films formed from archaebacterial lipids have resulted in membranes that are stable to temperatures in excess of 90°C (Gliozzi et al., 1983).

Although most studies of the ICS^{TM} biosensor have used antibody F_{ab} fragments as the receptor, the approach is generic and has been demonstrated to operate using oligonucleotide sequences, heavy metal chelates, and cell surface receptors. The specificity of the response is dependent on the receptor. A commercial device is under development and is primarily aimed at rapid, quantitative determination of time-critical diagnostic measures in whole blood. Operation of the device, however, is not constrained to just blood and could be used with any electrolyte containing biological fluid including serum, saliva, and urine.

18.4 Fabrication of a Membrane-Based Biosensor

Self-assembly of a stable membrane incorporating ion channels on a clean, smooth gold surface is possible using a combination of sulfur–gold chemistry and physisorption (Philp and Stoddart, 1996). The stages of biosensor fabrication are considered in the following sections.

Frances Separovic and Bruce A. Cornell

18.4.1 Preparation of Gold Surface

An initial step in the fabrication of a reliable biosensing device is the production of a molecularly smooth gold surface free of contaminants and oxides. An extensive literature exists on how to produce good quality gold surfaces and is briefly discussed here.

The quality of vapor-deposited and sputter-coated thin gold films on mica, heated in ultrahigh vacuum up to 500°C, has been reported (Guo et al., 1994). The gold surface, as shown by AFM, became atomically flat at 450–500°C. Surface contamination of the gold by organics and gold oxide was more significant in obtaining good high impedance films than simply the molecular smoothness of the gold. Grain boundaries in the "pebbled" gold surfaces observed in the nonannealed gold were suggested to capture impurities, which may cause leakiness in alkanethiol films. Immersion in hot piranha solution (H_2SO_4/H_2O_2) for 10–15 min, followed by electrochemical stripping of any resulting oxide resulted in gold that supports a high impedance self-assembled membrane (SAM).

Exposure to oxidants such as piranha solution, oxygen plasma or UV/ozone removes organic contaminants but causes the formation of gold oxide. Ron and Rubenstein (1994) discuss the risk of forming alkane thiol monolayers over preoxidized gold. Gold oxide may be removed by prolonged immersion in ethanol or by using electrochemical stripping. Failure to remove all traces of oxide prior to depositing an alkanethiol monolayer causes the oxide to be trapped beneath the alkanethiol film. As seen below, the ICS^{TM} sensor technology employs disulfides which requires rigor in eliminating gold oxide

Gold surfaces exposed to a laboratory atmosphere for only minutes were found by XPS to develop a layer of contamination approximately 0.6 nm thick composed of oxygen and carbon (Ron and Rubenstein, 1998). This problem was addressed by using an electrochemical technique, which oxidizes surface contaminants, cleans the surface of oxide and then accelerates the deposition of the alkane monolayer (Ron et al., 1998). Initially, the gold is electrochemically oxidized in water. At -0.3 V, the gold oxide is reduced in ethanol. Switching the potential at the gold to an oxidizing $+1.45$ V and by using a fast liquid exchange flow cell to synchronously introduce an alkanethiol into the solution a high quality, electrically sealing monolayer is formed in 1–2 s.

Alkanethiolates on gold, oxidize in air in the dark to form sulfinates and sulfonates. The kinetics of oxidation depends on the morphology of the underlying gold, increasing dramatically with a decrease in grain size and the amount of Au(111) on the surface and may explain the variation in the quality of alkanethiol SAM as reported by different groups (Lee et al., 1998). Grain boundaries of evaporated polycrystalline gold films were identified as an important catalytic site for oxidation. To prepare a smooth surface, the gold was annealed with a small butane flame. This cleaned the gold and facilitated its recrystallization into large regions of Au(111). "Epitaxially" grown gold surfaces were produced by slow (1 Å/s) thermal evaporation on "scratch free" mica at 2.5×10^{-7} mbar at 300°C until 100 nm of gold had been

deposited. The surface was transformed into defect free Au(111) over 150 × 150 nm areas. These regions were substantially more robust against oxidation and its effect on destabilizing electrical leakage of alkanethiol SAM.

The state of the gold surface and, in particular, the surface roughness is important for the reproducible formation of high quality self-assembled monolayers on gold. A pulsed potential pretreatment, which results in a twofold reduction in roughness of mechanically polished surfaces, has been reported (Hoogvliet et al., 2000). A flow cell and a 100 ms triple pulse sequence of +1.6, 0.0, and −0.8 V relative to a counter electrode are used. Pulsing for 2000–5000 s under flow conditions is required to achieve a smooth gold surface.

18.4.2 Formation of Tethered Bilayer Lipid Membrane

In order to increase the stability of the membrane, which forms the basis of the biosensor, a tethered monolayer of an alkane disulfide tethers the BLM to the gold electrode surface. In addition, a significant fraction of ether linked, membrane-spanning lipids are also tethered to the gold. These membrane-spanning lipids further stabilize the lamellar phase of the membrane lipids and possibly prevent insertion of additional material once the membrane is assembled. In our hands, these tethered membranes possess excellent stability over many months and can be stored dry and retain function when rehydrated for use.

18.4.2.1 Assembly of the Monolayer

The convenience and extensive experience available on sulfur–gold chemistry and tethering mechanism (Lingler et al., 1997) provide excellent groundwork for making a tethered BLM. The early literature on the formation of SAM of gold-tethered alkanethiols has been reviewed widely (Ulman, 1996).

The adsorption induced by Au_2O_3 interactions with polar species such as –OH, –COOH and $–PO_3H_2$ on the terminating groups of the SAM can cause serious packing disorder in the alkanethiol films (Tsai and Lin, 2001). This effect may be minimized by plasma, oxidizing the entire surface and then reducing it to metallic gold by ultrasonic agitation in oxygen free ethanol. Thus, the assembly process needs to be well controlled in order to achieve a reproducible SAM. Although disulfides have been detected, steric effects may play a significant role in the reduction of disulfides to thiols at gold surfaces. The major difference between disulfide and thiol SAM is in the kinetics of competitive film formation, which favors the thiols by 75:1 (Bain et al., 1989).

It is important to have control over the relative composition of the adsorbed film when fabricating devices based on SAM. The relationship between the composition of two-component SAM on gold and that of the solutions from which they were formed has been examined (Folker et al., 1994). A two-component monolayer of $HS(CH_2)_{21}CH_3$ and $HS(CH_2)_{11}OH$ was formed from solutions in ethanol. Phase separated monolayers were not observed: a single phase is preferred at equilibrium

for a two-component system of alkanethiols on gold, well equilibrated with alkane thiols in solution. Thus, under the ideal conditions of strongly cooperative film formation at the gold surface and equilibrium film growth, little or no control would exist over the relative ratios of component species in a mixed film on the gold. To counteract this effect, the film could be assembled under kinetic conditions and/or the cooperativity of the assembly process could be reduced. The ICS^{TM} biosensor membrane comprises phytanyl chain lipids and a substantial ethyleneglycol spacer group, and comprises four tethered species, which reduces the cooperativity of the film formation. The bulk and dynamic disorder of the phytanyl side chains result in a better seal against electrochemical stripping. The electrochemical sealing ability of the phytanyl groups further reduces the cooperativity of the film formation (Braach-Maksvytis and Raguse, 2000).

Potentially driven assembly of SAM favors the kinetic, metastable regime (Ma and Lennox, 2000). Self-assembled membrane formed under an applied potential produced an excellent seal in less than 10 min compared to no seal existing in the absence of a potential. Similarly, the composition of the binary film was uncontrolled without an applied potential but with 0.6 V applied to the gold during assembly, the composition was controlled in proportion to the relative concentration of the two components. Potential driven film formation can be used to create patterned SAM. An electrochemically directed adsorption process was used to selectively form SAM on one gold electrode in the presence of another nearby electrode (Hsueh et al., 2000). The monolayers formed were very similar to analogous SAM formed by chemisorption with added advantages of spatial control over coverage, short time required for coating (<1 min) and an ability to form SAM on gold that is not freshly evaporated. Difference in film properties across the gold surface are associated with lattice defects and oxide sites, at which thiol desorption is 2–3 times easier (Walczak et al., 1995).

During the self-assembly process, the sulfur atoms adopt an hexagonal lattice commensurate with the Au(111) structure but rotated 30° relative to the gold lattice (Dishner et al., 1996). The chains of the thiolates extend into space with the same all-*trans* conformation as observed in crystalline paraffins. Scanning Tunneling Microscopy studies have revealed that the chemisorption (presumably desorption) of the thiol is accompanied by the formation of 3–10 nm pits (Dishner et al., 1996). These pits can be eliminated by UV photolysis, which oxidizes the thiol to sulfonate and which can be rinsed from the surface with ethanol or water, leaving a smooth, pit-free surface. The pits, typically 3.3 nm diameter, involve nearly 100 gold atoms and represent approximately 10–15% of the surface area and are filled in by lateral diffusion of the gold. We have observed the introduction of gold in ethanol solutions resulting from soaking gold-coated slides in alkane-thiol and -disulfide containing solutions. Defect-free films have also been produced by heating SAM of *n*-octadecylthiol to almost the boiling point of ethanol at 77°C (Bucher et al., 1994) although no impedance measures were reported to indicate whether damage had occurred to the electrical seal of the film at these temperatures.

18.4.2.2 Assembly of the Lipid Bilayer

A number of reviews on the development of supported membranes are available (Sackmann, 1996; Meuse et al., 1998b). Stabilized BLMs have been prepared comprising an alkanethiol inner monolayer and a dimyristoylphosphatidylcholine, mobile outer layer (Meuse et al., 1998a). These structures have been termed hybrid bilayer membranes and may be formed from lipid vesicles or by transfer from air–water interfaces. These bilayers are noninterdigitated and possess a more ordered structure, equivalent to the effect of lowering temperature. Tethered and supported bilayer membranes have been generated from both thiolated and nonthiolated phospholipids (Steinem et al., 1996). Three techniques were employed: (1) the gold surface was initially covered with a chemisorbed monolayer of an alkanethiol such as octadecane thiol (ODT) or a thiolated phospholipid such as dimyristoylphosphatidyl-thiolethanolamine (DMPTE). A second lipid layer was deposited: (i) by Langmuir–Schaefer technique, (ii) from lipid solution in *n*-decane/isobutanol, (iii) by lipid–detergent dilution, or (iv) by fusion of vesicles; (2) charged molecules with thiol-anchors for attachment to the gold surface by chemisorption; or (3) direct deposition of lipid bilayer vesicles containing a thiolated phospholipid. The ion channel gA was codeposited using the second technique described above. Membrane capacitances of 0.55 μF/cm^2 $\pm$10% were obtained independent of the technique employed. Typically membrane seals were obtained to frequencies of $\sim$30 Hz and when doped with gA this was raised to $\sim$100 Hz.

Hybrid bilayers have been formed by the interaction of phospholipids with the hydrophobic surface of a self-assembled alkanethiol monolayer on gold (Meuse et al., 1998a). These membranes were characterized in air using atomic force microscopy, spectroscopic ellipsometry and reflection–absorption infrared spectroscopy. The added phospholipid was one monolayer thick, continuous, and exhibited molecular order similar to that seen in phospholipid bilayers. When characterized in water using neutron reflectivity and impedance spectroscopy, these hybrid bilayers possessed essentially the same properties as normal phospholipid bilayers, although the bilayer leakage level was not reported below 10 Hz. The capacitance of phospholipid/alkanethiol bilayers was found to closely mimic that obtained from solvent free phospholipid bilayers (Plant, 1993). The introduction of 10^{-6}M melittin, a pore-forming peptide, changed the bilayer from being impermeable to being highly conductive.

A biosensor based on a supported bilayer membrane was proposed (Stelzle et al., 1993). Positively charged vesicles of dioctadecyldimethylammonium bromide were fused to form a supported bilayer membrane on a monolayer of a carboxy mercaptan, which was deposited onto a 100 nm thick evaporated gold film on a silanized glass substrate. Impedance spectroscopy (2000–1 Hz) revealed sealing membranes down to $\sim$100 Hz, at which point defects in the membranes required a more complex network to explain the data. A tethered BLM on a silicon oxide surface or membrane on a chip has been described recently and included functional gA channels (Atanasov et al., 2005).

18.4.3 Membrane Components

The chemistries of the species making up the lipid membrane of the ICS™ biosensor have been described (Raguse et al., 1998; Burns et al., 1999a,b,c; Raguse et al., 2000; Anastasiadis et al., 2001). Representative examples of the membrane components are shown in Fig. 18.2. These include two classes of compounds: one that is tethered to the gold surface and another that is physically absorbed to the surface but free to diffuse in the plane of the membrane.

Typically, the concentration used is 350 μM of **1** and 2 mM for **5**; while the mole ratios of **1**:**2**(R_1):**2**(R_2):**3** are 40,000:400:1:1 and for **5**:**6**:**4** are 28,000:12,000:1. Attachment of the membrane to the gold substrate is via a disulfide moiety in **1**–**3**. The disulfide compound acts as a tether and includes a benzyl spacer group that reduces the 2D packing density of the assembled membrane. The lower packing density acts to facilitate the entry of ions into the space between the gold surface and the membrane, or the reservoir, which is discussed further below. As discussed above, the phytanyl chain lipids used here are chemically stable at high temperatures (Stetter, 1996), and the bulky methyl substituents reduce the temperature dependence of the membrane disorder around the normal operating temperatures for the biosensor of 20–30°C. The phytanyl chains also provide an excellent electrical seal based on impedance measurements. Biphenyl linkers at the mid-plane of the bilayer, **2**, adds rigidity and prevents the membrane spanning lipids entering and emerging on the same side of the membrane (Kang et al., 1999).

Another series of tether compounds are shown in Fig. 18.3. The C11 series (compound **7**) have both the sulfur attachment chemistry and the van der Waals attraction of the C11 sequence for each other, giving additional binding energy and protection to the gold surface from the electrolyte solution. The reduction in surface charge also significantly alters the reservoir performance. The all-ether reservoir linkers in compounds **7** and **8** replace the succinate groups of **1–4** and eliminate instabilities that can arise from the hydrolysis of ester groups. The all-ether reservoir significantly extends the storage lifetime of the membrane as well as improving the reservoir properties.

The area per lipid molecule is determined by a number of contributions, including the gold–sulfur interface, the spacer molecules, and the interaction of the hydrocarbon chains within the membrane. Membrane spanning lipids such as **2** and half membrane spanning lipids such as **1, 5** and **6** are mixed in different ratios to adjust the membrane packing. The packing within the membrane may also be adjusted using compounds such as **9** and other spacer molecules such as dodecanethiol.

18.4.4 The Gramicidin A Ion Channel

Gramicidin A is a pentadecapeptide (1882 Da) produced by the soil bacteria *Bacillus brevis* (Katz and Demain, 1977). An extensive literature exists on the ion transport properties of the linear gramicidins (Koeppe and Andersen, 1996; Wallace, 1998). The conformation of gramicidin ranges from random coil to a family of intertwined

Tethered species

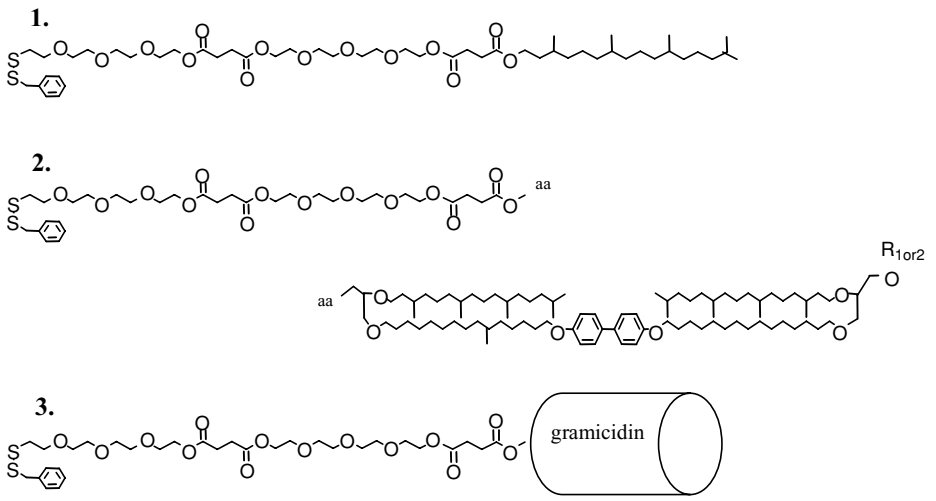

Mobile species

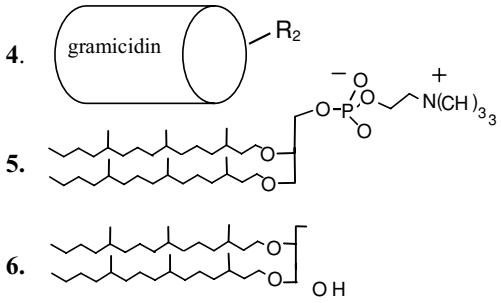

Where for both mobile & tethered species:

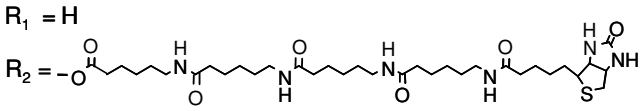

Fig. 18.2 Chemical structures of components that form the tethered BLM. Compounds **1–3** are tethered species while **4–6** are mobile. A minor portion of **2** and all of **4** are linked to R_2, an aminocaproyl-linked biotin.

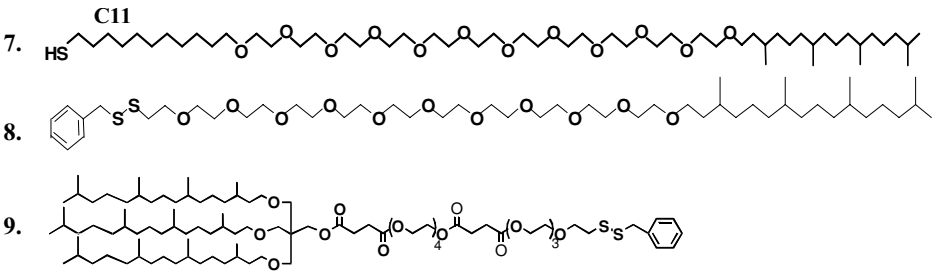

Fig. 18.3 Additional tethered compounds used in assembly of the BLM.

helices, depending on the solvent. However, in a lipid bilayer lipid gA forms a single coil, right-handed $\beta^{6.3}$ helix, anchored at the lipid–water interface by four tryptophans in positions 9, 11, 13, and 15 at the C terminus. The structure is further stabilized by nine internal hydrogen bonds between the adjacent turns of the helix, made possible by the alternating L-D amino-acid sequence. The conducting form of gA is an *N–N* dimer of $\beta^{6.3}$ helices, which forms six hydrogen bonds stabilizing the dimer across the hydrocarbon core of the BLM. Gramicidin selectively facilitates the transport of monovalent cations across the bilayer (Myers and Haydon, 1972).

Unlike large mammalian channels, gA is very stable both chemically and structurally. Gramicidin can be modified using synthetic organic chemistry techniques and can spontaneously fold into the ion conducting form when incorporated into a BLM. Below mM concentrations in ethanol gA has a random coil structure and converts to the $\beta^{6.3}$ helix in a BLM. It is important to ensure that gA has not been transferred from a solvent such as dioxane, which may require many hours to convert from the conformation adopted in dioxane to the channel form.

Many analogues of gA have been synthesized. In order to utilize gA as an ion channel switch it is necessary to attach linkers for both the tethered and the mobile species. The linkers are attached to the ethanolamine hydroxyl group and have been mainly variants on aminocaproyl and tetraethyleneglycol groups for the mobile and tethered gA, respectively. Provided the linker attachment was to the C terminus ethanolamine hydroxyl, the conductance fell within a range of approximately $\pm$ 10% of the native gA (Fig. 18.4). Modifications too near the channel entrance can eliminate conduction. Similar "C" terminus biotin labeled gA has been reported (Suarez et al., 1998; Separovic et al., 1999; Anastasiadis et al., 2001) and we have shown that biotinylated gA analogues preserve essentially the same 3D structure of native gA (Separovic et al., 1999; Cornell et al., 1988).

18.4.5 Receptor Component: Antibody Fragments

Rather than using whole antibodies, which can cause species cross reactivity, F_{ab} fragments are used in the ICS^{TM} biosensor. Antibodies are enzymatically cleaved at the hinge region and biotinylated. The F_{ab} fragments are attached to the membrane using a streptavidin–biotin complex. Although other linker chemistries have proven

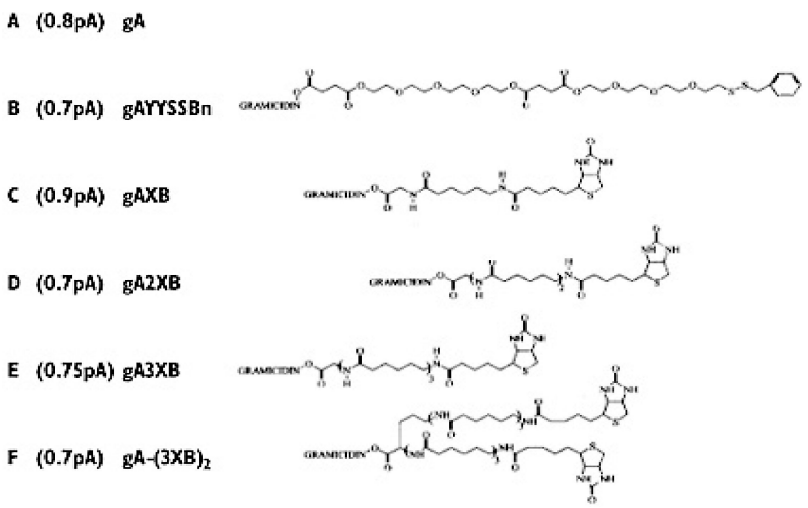

Fig. 18.4 Examples of native (A) and modified gramicidins containing: (B) tetra-ethylene glycol, or (C–F) aminocaproyl linker groups. The single channel current is shown in parenthesis adjacent to each structure.

satisfactory for certain applications, the streptavidin–biotin linkage is convenient and readily available.

18.4.6 Assembly of the Biosensor

In the ICS^{TM} biosensor the bilayer membrane is assembled during an ethanol/water rinse as shown schematically in Fig. 18.5. Assembly of the biosensor depends on forming a stable BLM using a tethered hydrocarbon layer on a gold substrate to achieve a tight bonding.

18.5 Mechanism of Operation

Although there have been many attempts to engineer receptor-based gated ion channels, the proposed mechanisms have had a limited range of applications and require reengineering for each new analyte. Gating mechanisms include molecules that block the channel entrance (Lopatin et al., 1995) and antichannel antibodies that disrupt ion transport (Bufler et al., 1996). Whilst the ICS^{TM} biosensor uses ion channel transduction, however, it is able to be adapted to detect many different classes of target.

18.5.1 Detection of Large Analytes

The large analyte class includes microorganisms, proteins, polypeptides, hormones, oligonucleotides, and DNA segments. If a suitable antibody pair is available, the

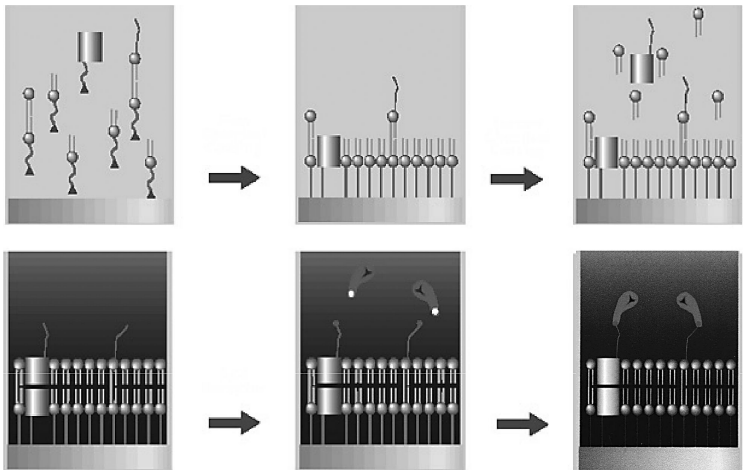

Fig. 18.5 A fresh gold surface is exposed to an ethanol solution of the tethering species **1**–**3**, for 10 min, which produces the inner and part of the outer monolayer of the BLM. After an alcohol rinse, a second ethanol solution of the mobile membrane species, **4** and **5**, is added. A lipid bilayer structure forms spontaneously when rinsed with water. Some lipids span the membrane, whilst others are mobile within the membrane plane. Antibody fragments are then added in the aqueous solution and attached using a streptavidin–biotin linkage (as shown in Fig. 18.1). For large analyte detection, which involves a "sandwich assay" configuration, an equimolar mixture of the two antibody fragments is added.

biosensor may be adapted to the detection of any antigenic target. The ion channel gA is assembled into a tethered lipid membrane and coupled to an antibody targeting a particular compound of diagnostic interest. Analyte binding causes the gA channels to switch from predominantly conducting dimers to predominantly nonconducting monomers (Fig. 18.6). A competitive assay has also been devised in which the analyte causes the population of channel dimers to increase.

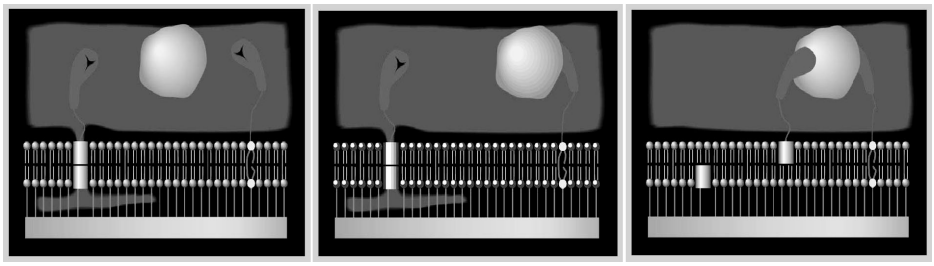

Fig. 18.6 Analyte binding to the antibody fragments causes the conformation of gA to shift from conducting dimers to nonconducting monomers, which causes a loss of ion conduction across the membrane. Scale = 5 nm.

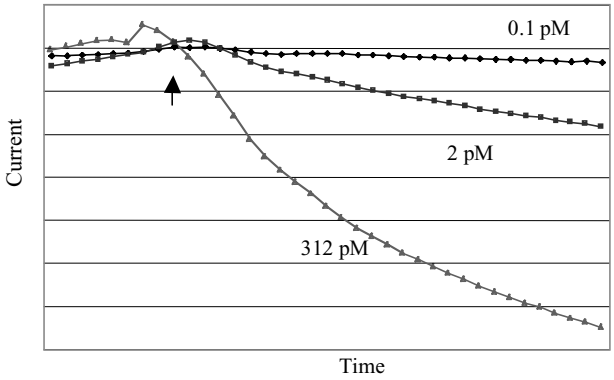

Fig. 18.7 Biosensor response to Thyroid Stimulating Hormone (TSH) over the initial 300 s following analyte addition (arrow).

18.5.2 Examples of Operation

(i) *Thyroid Stimulating Hormone* (TSH) is a 28 kDa protein with α and β subunits to which a matched pair of antibodies is used, each targeting different nonoverlapping epitopes. The biosensor response to TSH is shown in Fig. 18.7.

(ii) *Ferritin* is the principal iron transporting protein in human serum and, having a molecular weight of ∼450 kDa, is one of the largest soluble proteins regularly measured clinically. With 24 equivalent subunits each accessible to cross-linking, only a single F_{ab} type is required to elicit a response. Figure 18.8 shows a titration curve of the biosensor response to ferritin in patient serum.

A comparison of the results of the ICS^{TM} biosensor with a Diagnostics Products Corporation (Los Angeles, CA) analyzer for measuring ferritin concentration in the serum taken from 100 patients in given in Fig. 18.9. The biosensor performs well over a wide range of analyte concentrations under clinical conditions.

18.5.2.1 Performance Considerations

Assuming an adequate mass transport of analyte to the membrane and that the surface density of tethered antibodies significantly exceeds that of antibodies linked to the mobile channels, the idealized behavior of the biosensor may be modeled by a family of coupled equations. The 2D reactions on the membrane surface are generally faster than the 3D reaction rates between the analyte in solution and the surface (Hardt, 1979). Thus for low and medium analyte concentrations, the 3D processes will be rate limiting while at high concentrations, 2D processes will become important. A further limiting condition is the lifetime of the dimeric channel. It is thus straightforward to numerically simulate the device behavior for large analyte detection (Woodhouse et al., 1999; Cornell, 2002). The quantitative measure of analyte concentration may be taken as the initial rate of current increase. At low analyte concentrations 2–3 decades of linear response to analyte are available while at higher concentrations,

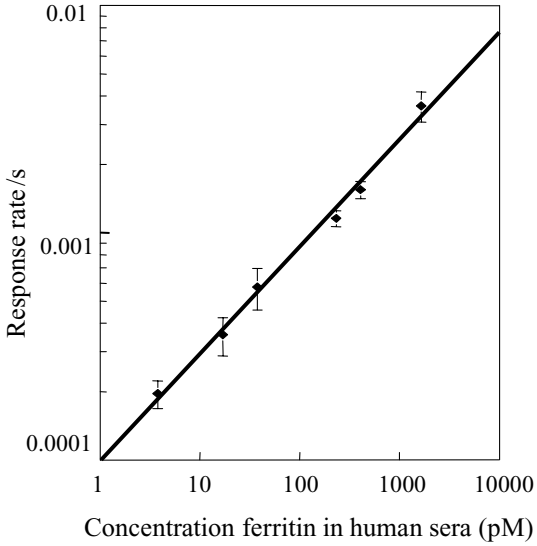

Fig. 18.8 Biosensor response rate for a range of concentrations of ferritin in human serum. The rate is obtained by normalizing the initial slope of the response curve to the initial admittance. The initial slope of the response is obtained within the first 180–300 s depending on the analyte concentration.

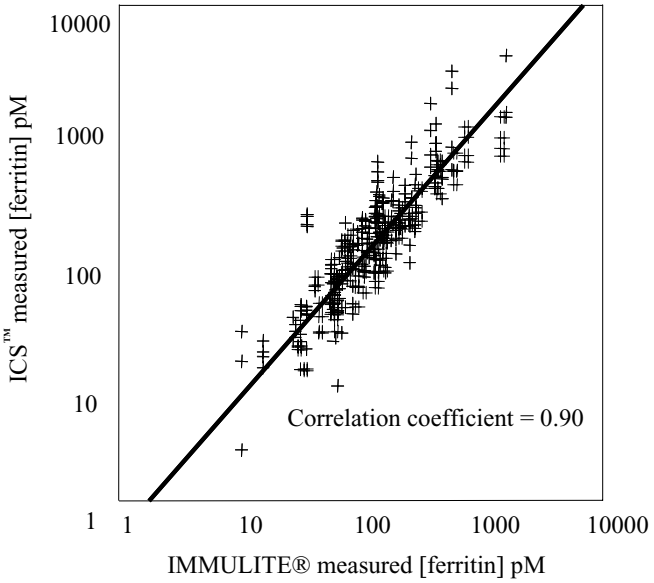

Fig. 18.9 A comparison of estimated ferritin concentrations from 100 patients measured by the ICS™ biosensor and a Diagnostics Products IMMULITE® analyzer. The measurements were made in serum at 30°C. The patients were chosen to provide a wide spread of clinical values.

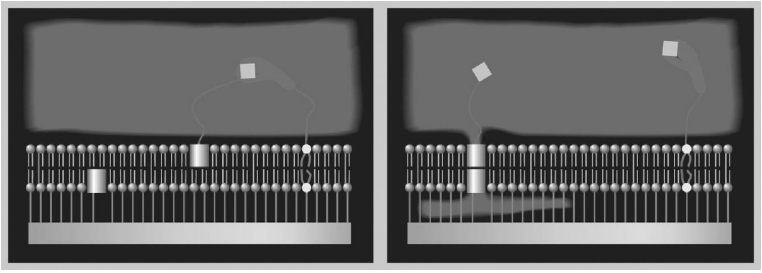

Fig. 18.10 Small analyte detection: the mobile channels are cross-linked to anti-digoxin F_{ab} anchored at the tether sites in the absence of analyte (e.g. digoxin). Dimer formation is prevented and the conductance of the membrane falls. The introduction of analyte competes off the hapten (digoxin analogue) and increases the membrane conductance.

approaching nanomolar, the gA dimer lifetime or the cross-linking rate of the mobile ion channels to the tethered antibodies will be limiting.

The variables available in establishing the biosensor operating conditions are: the surface density of tethered antibody sites $[T]$, the surface density of antibodies attached to mobile channels $[G_M]$, and the "on rate" of the chosen antibody k_{3D}. The "on rate" of the antibodies attached to the mobile channels in general need not be as large as those on the primary tethered capture sites $[T]$ since 2D processes are more effective. The ratio $[T]/[G_M]$ "amplifies" the apparent capture rate of analyte $[A]$ from what would otherwise be the simple first order rate constant, $k_{3D}[A]$ to $k_{3D}[A][T]/[G_M]$. The maximum amplification in this configuration approaches 10^2–10^3 and is dependent on the length of the linkers and whether streptavidin has been used as a coupling protein. At higher analyte concentrations, in the range nM–μM, the amplification may be adjusted downwards by lowering the $[T]/[G_M]$ ratio. With the introduction of flow, 1μL/min, to the analyte stream the mass transfer limitation can be overcome and the capture density $[T]$ increased by an order of magnitude with a proportionate increase in the response.

18.5.3 Detection of Small Analytes

For low molecular weights analytes such as therapeutic drugs where the target is too small to use a two-site sandwich or cross-linking assay, a competitive adaptation of the ICS™ biosensor is available (Fig. 18.10). In this case the biosensor conduction increases when the analyte binds.

18.5.3.1 Small Analyte Response

The ICS™ system has been configured for the cardiac stimulant digoxin (781 Da) linked at the 3′ position to gramicidin through a flexible tetra-aminocaproyl group. During fabrication when the biotinylated F_{ab} fragment is added, the conduction is reduced due to cross-linking of mobile gA-digoxin with tethered antibody fragments.

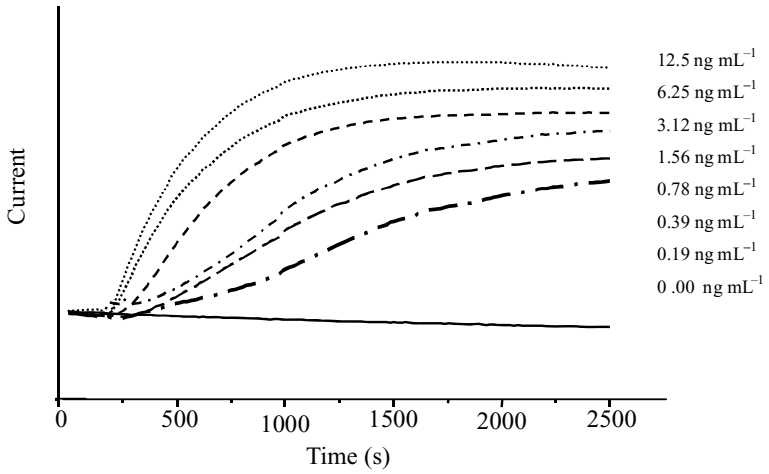

Fig. 18.11 Biosensor reponses to a range of digoxin concentrations that span the clinical range of ∼1 ng/mL.

The addition of digoxin displaces the gA-digoxin and the conduction increases (Fig. 18.11).

18.5.3.2 Performance Considerations

Competition for the tethered antibodies $[T]$ between analyte and hapten on the mobile gA $[G^{\mathrm{h}}_{\mathrm{M}}]$ establishes an equilibrium, which determines the surface density of the complex $[T^{*}\, G^{\mathrm{h}}_{\mathrm{M}}]$. As with the large analyte example, the current output from the sensor is determined by the surface density of gramicidin dimers $[G_{\mathrm{D}}]$. The quantitative measure of analyte concentration may be taken as the initial rate of current increase or the endpoint gating ratio (Fig. 18.12). With the competitive, small analyte system, the 'amplification' effect described above is not available (Woodhouse et al., 1999). However, it is possible to adjust the biosensor sensitivity over a considerable range by manipulation of component surface densities.

18.5.4 Biosensor Applicability

The ICS$^{\mathrm{TM}}$ biosensor has a wide range of applications based on a common transduction mechanism. Over 50 different antibodies as well as extracellular cell surface receptors for growth factor detection, oligonucleotide probes for DNA strand detection, lectins for glucose detection, and metal chelates for heavy metal detection have been utilized in the ICS$^{\mathrm{TM}}$ biosensor. The major requirement is an attachment chemistry that will not inactivate the receptor for a particular analyte. Figure 18.13 shows the biosensor response to a range of analytes.

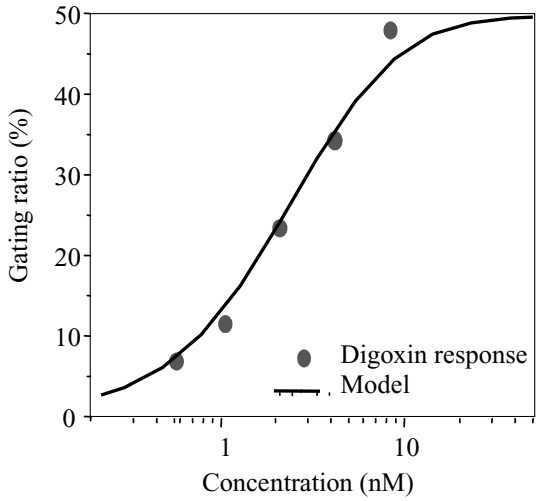

Fig. 18.12 Endpoint gating ratios, i.e., % change in conduction upon the addition of digoxin at various concentrations shown superimposed on a numerical model (Woodhouse et al., 1999). The response time is essentially fixed by the off rate $k^{-1}A^h$ of the hapten from the F'_{ab}, which for the present example of digoxin is ≈50 s.

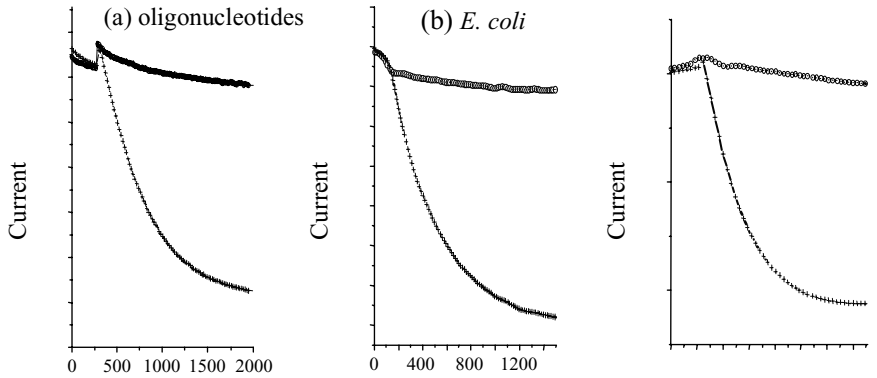

Fig. 18.13 Biosensor responses to different classes of target analyte: (a) 19-base oligonucleotide probe biotinylated at the 5′ end via a 23 atom phosphoamidase linker. The response to a 5 nM challenge of a 52-mer target sequence is shown. The double stranded target was heated to 95°C and cooled to ∼60°C. The biotinylated probe on the gA hybridized faster than its complementary sequence resulting in the gating shown. (b) Biotinylated F_{ab} directed to *E. coli* following a challenge of 10^5 cells/mL. (c) Biotinylated complementary pair of F_{ab} directed to two epitopes on the α subunit of TSH after addition of 100 pM TSH. The upper curve is a control using an anti-theophylline antibody and the lower is the active measure.

Frances Separovic and Bruce A. Cornell

18.6 Biosensor Characterization

18.6.1 Ellipsometry

Ellipsometry was used to determine the biosensor membrane thickness. Direct calibration using alkane thiols from C_8 to C_{18} yielded a thickness for the BLM of 4 nm. The thickness of the mobile outer layer was determined to be 2 nm by rinsing off the layer with ethanol. This is close to the value expected for a fluid monolayer. The overall thickness of the tethered BLM was measured to be ∼12–15 nm, although in estimating this value assumptions are made of the dielectric constant for a tethered membrane separated from the gold electrode by a polar linker.

18.6.2 Impedance Spectroscopy

The membrane thickness can also be determined from the membrane capacitance, C_m, based on modeling the impedance spectrum over a frequency range swept over typically 0.1–1000 Hz. Both the phase and modulus are measured and fitted. The electrical equivalent circuit of a tethered BLM is shown in Fig. 18.14. Simple RC networks provide a fit with <2% residual. A measured membrane capacitance of 0.5 μF/cm^2 was obtained and, assuming a relative dielectric constant of 2.2 for the membrane chains, gives an overall membrane thickness of ∼4 nm.

The validity of this equivalent circuit as a good description of the conductive tethered BLM is shown in Fig. 18.15, which shows the impedance profile and phase relationship.

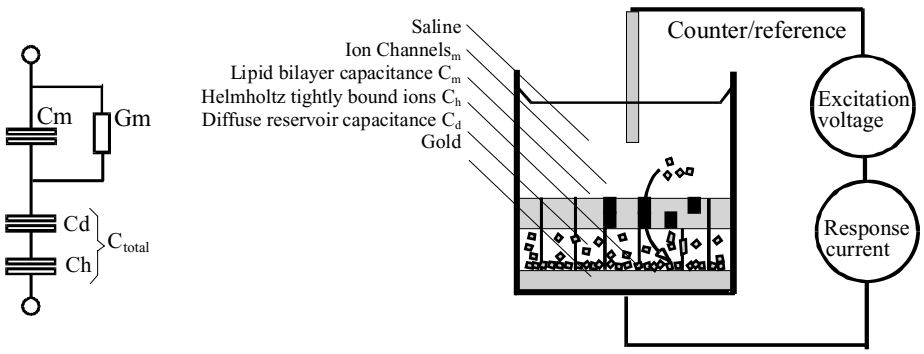

Fig. 18.14 Equivalent electrical circuit used to characterize the tethered BLM (Krishna et al., 2001). The main elements are the conduction G_m, which describes the ion flow across the membrane dominated by the gramicidin channels, the membrane capacitance $C_{m,}$ the Helmholtz capacitance C_h of ions crowding against the gold electrode, and the diffuse capacitance C_d of ions within a concentration cloud decaying back into the reservoir space. For an excitation of typically 50 mV the equivalent circuit may be approximated as an effective Helmholtz capacitance, C_h of 3.5 μF/cm^2, in series with a membrane capacitance of 0.6 μF/cm^2.

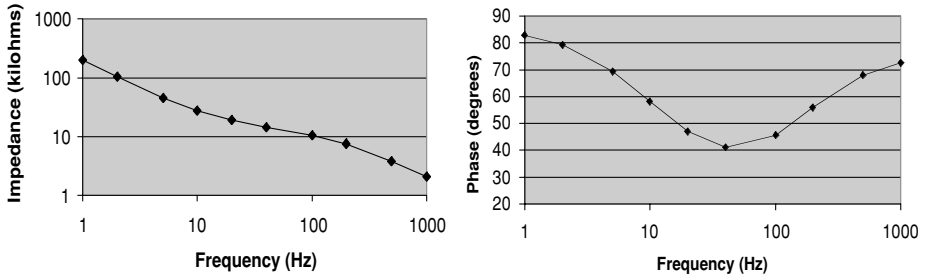

Fig. 18.15 The impedance of a capacitor varies according to $Z = 1/2\pi fC$. A plot of $\log_{10} Z$ against $\log_{10} f$ yields a linear relationship with a slope of -1 and an intercept at $1/2\pi$Hz of $\log_{10} C$. (Left): At high frequencies $C \approx C_m$ and at low frequencies $C \approx C_h$ where C_m and C_h refer to the capacitance of the membrane and Helmholtz layers, respectively. The frequency at which the impedance profile crosses from C_m-dominated to C_h-dominated behavior follows the change in G_m arising from the ion channels. (Right): The crossing point is conveniently identified by the frequency f_ϕ at which the phase angle ϕ between the excitation and the resultant current is minimized.

18.6.3 Membrane Composition

When fabricating self-assembling systems an important issue is to determine and control the ratio of components in the film. Many factors influence the membrane configuration including the composition of the coating solutions, the condition of the surface, and the conditions under which the deposition occurs. A useful measure available in the gA-based system is the ability to measure directly the ratio of gramicidin to nongramicidin species within the film, based on changes in the electrical conductivity, e.g., G_m can be titrated against the gA concentration in the depositing solution. The conduction is found to be dependent on the insertion of gA into the inner, outer, or both layers. The derived K_{2D} for the gramicidin monomer–dimer interaction was $7 \times 10^9 \text{cm}^{-2}$ if the inner layer gramicidins are taken as reference and $1 \times 10^9 \text{cm}^{-2}$ if the outer layer gramicidins are taken as reference (Cornell, 2002). This suggests that the tethered gA surface density is lower than nominal, although absolute estimates of the membrane composition require other techniques such as radiolabeling.

18.6.4 Characterization of the Reservoir

The conductance of the tethered BLM assembled from the compounds shown in Fig. 18.2 is insensitive to ion type, indicating that it is not limited by the conductivity of the gA channel. The reservoir properties, however, dominate the ion channel conduction. The linker composition of the reservoir significantly influences the magnitude and properties of the diffuse layer capacitance (Krishna et al., 2001) and the magnitude and voltage dependence of the apparent ion channel conductance. The ion channel conductance appears to be a factor of 8–10 greater for the all-ether reservoirs (compound **8** in Fig. 18.3). Spacer molecules improve the apparent channel

conduction but also add complexity to the coating solutions and introduce variation in the composition of the tethered BLM.

The application of a 100–300 mV potential, negative on the gold electrode, improves the ability of the all-ether and succinate-linked reservoirs to store ions, and increases the apparent conductivity of the ion channels. The dependence on potential of the reservoir species with the C11 linkers is much reduced, in proportion to the lowered surface charge at the gold arising from the C11 coating. As described earlier, additional advantages that result from using the C11 family of compounds is the protection of the sulfur–gold surface against chemical degradation from the test solution and a greater stability of the attachment chemistry. The C11–C11 groups interact through van der Waals forces adding to the sulfur–gold interaction. As a result, the C11 family of compounds is the preferred attachment chemistry for long-term storage of the ICS^{TM} biosensor.

18.6.5 Nonspecific Binding

Ellipsometry was used to determine the level of nonspecific binding to the tethered BLM, using streptavidin–biotin as a model for binding on the surface. The effect of surface type on nonspecific binding of 42 nM streptavidin was examined (Cornell, 2002). A tethered bilayer of predominantly a 70:30 mix of compounds **5** and **6** in Fig. 18.2 resulted in binding below the level of detection. A substantial fraction of phosphatidylcholine groups within the tethered bilayer surface significantly reduces nonspecific binding of streptavidin. When biotinylated lipids are included in the BLM, the apparent thickness of the film progressively increases reflecting the binding of streptavidin to the membrane surface, i.e., specific binding increases linearly with the inclusion of biotinylated lipids. The low nonspecific binding characteristics of the phosphatidylcholine headgroup tethered BLM results in an ability to detect target analytes in whole blood without prepreparation of the sample and minimal matrix effects (Fig. 18.16).

18.6.6 BLM Stability

The stability of the tethered BLM depends on several factors including the lifetime of the sulfur–gold bond, the chemical stability of the various linkers, and the ability of the membrane to resist mechanical damage and loss of the mobile outer layer. The use of a C11 segment with a thiol or disulfide species (compound **7** in Fig. 18.3) provides substantial additional retention of the monolayer components. Assemblies of thiols employing the C11 sequence are able to withstand extensive storage in ethanol at 50°C with no loss of material to solution compared to films without C11, which lost a substantial amount (Cornell, 2002). Replacement of succinate by all ether linkers (compound **8** in Fig. 18.3) has a further substantial effect on the stability of the membrane. The sealed membranes fabricated from the ether linkers are stable beyond 3 months when fully hydrated.

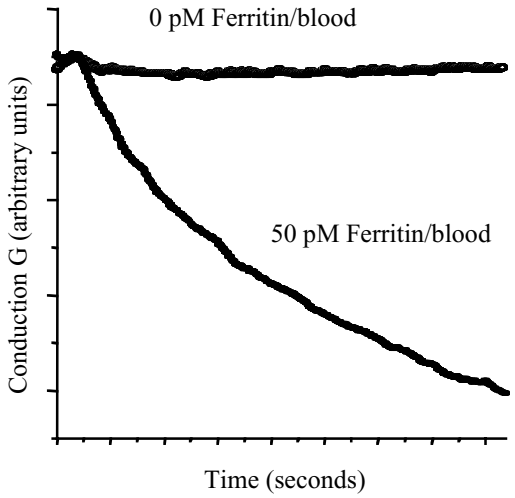

Fig. 18.16 Biosensor response to whole blood containing 50 pM ferritin compared to a control without ferritin.

A further strategy for stabilizing the biosensor is to return function on rehydrating a fully assembled, freeze-dried sensor. Following rehydration sensor function returns. This requires assembling a hydrated sensor up to the stage where analyte is to be added. The biosensor is rinsed with a storage solution and is then freeze dried. Freezing a fully hydrated sensor also appears to cause no loss of function upon being returned to operating temperature (DARPA report, 2001). Under these circumstances no cryoprotectants are needed and excellent recovery has been obtained with phosphate-buffered saline. These approaches can be used for the long-term storage of BLM devices.

18.7 Further Developments

Major opportunities in technology developments using BLM include miniaturization and patterning. Nanometer-sized gold electrodes have been made by using nm size latex spheres as a lift-off mask (Padeste et al., 1996). Cell adhesion and growth can be controlled with micro-patterned supported BLM by using phosphatidylserine to specify regions for growth of cells (Groves et al., 1997, 2000). Patterned SAM have been formed by patterning the topography of their metallic supports (Aizenberg et al., 1998), while microcontact printing of lipophilic SAM has been used for the attachment of biomimetic lipid layers to surfaces (Jenkins et al., 1999). Microstructures of solid-supported lipid layers have been made using SAM pattern by scanning electrochemical microscopy (Ufheil et al., 2000) and techniques for rapid prototyping and production of nanometer-sized arrays have been described (Fan et al., 2000).

Once a microarray has been produced, the arrays can be patterned with selected functionalities. The ICS^{TM} biosensor is able to employ a technique in which the streptavidin–biotin linker is blocked unless irradiated by UV. The irradiation can be applied through a patterned mask to permit streptavidin attachment to selected sites so that UV irradiation is used to selectively deprotect biotin sites and permit their functionalization using a streptavidin–biotin attachment.

A range of functionalities has been incorporated within tethered BLM, including peptide nanotubes (Motesharei and Ghadiri, 1997), crown ethers (Terrettaz et al., 1998), antigenic peptides (Scheibler et al., 1999), and the Ompf porin channel (Stora et al., 1999). Cytochrome C has been incorporated into a tethered membrane as one of the first examples of a functionally active biomimetic surface (Naumann et al., 1999). A chip-based sensor using etched silicon has been fabricated to measure single state currents of alamethicin (Schmidt et al., 2000), while the pore-forming toxin α-hemolysin has been reconstituted in supported bilayers (Glazier et al., 2000). Although the detection of single ion channel currents has not yet been reported, with the reduction of electrode dimensions to the micrometer scale, however, single channel noise from gA can be detected in tethered BLM. The combination of miniaturization and selective patterning can lead to higher sensitivities and detection of multiple analytes.

Acknowledgments

This work was in part supported by the Cooperative Research Centre for Molecular Engineering. Ambri Ltd. has licensed certain fields of application of the Ion Channel Switch technology to Biosensors Enterprise Ltd. (BEL). BEL has undertaken further development of the technology with Ambri. BEL is a joint venture between Dow Corning and Genencor International.

References

Aizenberg, J., A.J. Black, and G.M. Whitesides. 1998. Controlling local disorder in self-assembled monolayers by patterning the topography of their metal supports. *Nature* 394:868–871.

Anastasiadis, A., and F. Separovic. 2003. Solid-state NMR structural determination of components in an ion channel switch biosensor. *Aust. J. Chem.* 56:163–166.

Anastasiadis, A., F. Separovic, and J. White. 2001. Synthesis of deuterated aminocaproyl linkers. *Aust. J. Chem.* 54:747–750.

Atanasov, V., N. Knorr, R.S. Duran, S. Ingebrandt, A. Offenhausser, W. Knoll, and I. Koper. 2005. Membrane on a chip: A functional tethered lipid bilayer membrane on silicon oxide surfaces. *Biophys. J.* 89:1780–1788.

Bain, C.D., J. Evall, and G.M. Whitesides. 1989. Formation of monolayers by the coadsorption of thiols on gold: Variation in the head group, tail group, and solvent. *J. Am. Chem. Soc.* 111:7155–7164.

Braach-Maksvytis, V., and B. Raguse. 2000. Highly impermeable 'soft' self-assembled monolayers. *J. Am. Chem. Soc.* 122:9544–9545.

Bucher, J.-P., L. Santesson, and K. Kern. 1994. Thermal healing of self-assembled organic monolayers: Hexane- and octadecanethiol on Au(111) and Ag(111). *Langmuir Lett.* 10:979–983.

Bufler, J., S. Kahlert, S. Tzartos, K.V. Toyka, A. Maelicke, and C. Franke. 1996. Activation and blockade of mouse muscle nicotinic channels by antibodies directed against the binding site of the acetylcholine receptor. *J. Physiol. (Lond.)* 492:107–114.

Burns, C.J., L.D. Field, K. Hashimoto, B.J. Petteys, D.D Ridley, and M. Rose. 1999a. Synthesis of steroisomerically pure mono-ether lipids. *Aust. J. Chem.* 52:387–396.

Burns, C.J., L.D. Field, K. Hashimoto, B.J. Petteys, D.D. Ridley, and S. Sandanayake. 1999b. A convenient synthetic route to differentially functionalized long chain polyethylene glycols. *Synthetic Comm.* 29:2337–2347.

Burns, C.J., L.D. Field, J. Morgan, D.D. Ridley, and V. Vignevich. 1999c. Preparation of cyclic disulfides from bisthiocyanates. *Tetrahedron Lett.* 40:6489–6492.

Cornell, B.A. 2002. Membrane-based biosensors. *In*: Optical Biosensors. F.S. Ligler and C.A. Rowe Taitt, editors. Elsevier Science B.V., Amsterdam, pp. 457–495.

Cornell, B.A., V.L.B. Braach-Maksvytis, L.G. King, P.D. Osman, B. Raguse, L. Wieczorek, and R.J. Pace. 1997. A biosensor that uses ion-channel switches. *Nature* 387:580–583.

Cornell, B.A., F. Separovic, R. Smith, and A.J. Baldassi. 1988. Conformation and orientation of gA in oriented phospholipid bilayers measured by solid state carbon13 NMR. *Biophys. J.* 53:67–76.

De Rosa, M., A. Gambacorta, B. Nicolaus, B. Chappeand, and P. Albrecht. 1983. Isoprenoidethers: Backbone of complex lipids of the archaebacterium *Sulfolobus solfataricus*. *Biochim. Biophys. Acta* 753:249–256.

DARPA Report number N65236-98-1-5412. 2001.

Dishner, M.H., F.J. Feher, and J.C. Hemminger. 1996. Formation and photooxidation of n-dodecanethiol self-assembled monolayers on Au(111): 'Pits' formed during chemisorption disappear upon oxidation *J. Chem. Soc. Chem. Comm.* 1971–1972.

Fan, H., Y. Lu, A. Stump, S.T. Reed, T. Baer, R. Schunk, V. Perez-Luna, G.P. López, and C.J Brinker. 2000. Rapid prototyping of patterned functional nanostructures. *Nature* 405:56–60.

Folker, J.P., P.E. Laibinis, G.M. Whitesides, and J. Deutch. 1994. Phase behavior of two-component self-assembled monolayers of alkanethiolates on gold. *J. Phys. Chem.* 98:563–571.

Glazier, S.A., D.J. Vanderah, A.L. Plant, H. Bayley, G. Valincius, and J.J. Kasianowicz. 2000. Reconstitution of the pore-forming toxin, α-hemolysin, in phospholipid/1-thiahexa(ethylene-oxide) alkane-supported bilayers. *Langmuir* 16:10428–10435.

Gliozzi, A., R. Rolandi, M. De Rosa, and A. Gambacort. 1983. Monolayer black membranes from bipolar lipids of archaebacteria and their temperature-induced structural changes. *J. Membr. Biol.* 75:45–56.

Groves, J.T., L.K. Mahal, and C.R Bertozzi. 2001. Control of cell adhesion and growth with micropatterned supported lipid membranes. *Langmuir* 17:5129–5133.

Groves, J.T., N. Ulman, and S.G. Boxer. 1997. Micropatterning fluid lipid bilayers on solid supports. *Science* 275:651–653.

Guo, L.H., J. Facci, R. Moser, and G. McLendon. 1994. Reactivity of alkanethiols toward gold films deposited on silica and mica.*Langmuir* 10:4588–4593.

Hardt, S.L. 1979. Rates of diffusion controlled reactions in one, two, and three dimensions. *Biophys. Chem.* 10:239–243.

Hoogvliet, J.C., M. Dijksma, B. Kamp, and W.P. van Bennekom. 2000. Electrochemical pretreatment of polycrystalline gold electrodes to produce a reproducible surface roughness for self-assembly: A study in phosphate buffer pH 7.4. *Anal. Chem.* 72:2016–2021.

Hsueh, C.C., M.T. Lee, M.S. Freund, and G.S. Ferguson. 2000. Electrochemically directed self-assembly on gold. *Angew. Chem. Int. Ed. Engl.* 39:1227–1230.

Jenkins, A.T.N., N. Boden, R.J. Bushby, S.D. Evans, P.F. Knowles, R.E. Miles, S.D. Ogier, H. Schoenherr, G.J. Vancso. 1999. Microcontact printing of lipophilic self-assembled monolayers for the attachment of biomimetic lipid bilayers to surfaces. *J. Amer. Chem. Soc.* 121:5274–5280.

Kang, J.F., A. Ulman, and R. Jordan. 1999. Mixed self-assembled monolayers of highly polar rigid biphenyl thiols. *Langmuir* 15:2095–2098.

Katz, E., and A.L. Demain. 1977. The peptide antibiotics of Bacillus: Chemistry, biogenesis and possible functions. *Bacteriol. Rev*. 41:449–474.

Koeppe, R.E., and O.S. Andersen. 1996. Engineering the gramicidin channel. *Ann. Rev. Biophys. Biomol. Struct.* 25:231–258.

Krishna, G., J. Schulte, B.A. Cornell, R. Pace, L. Wieczorek, and P.D. Osman. 2001. Tethered bilayer membranes containing ionic reservoirs: The interfacial capacitance. *Langmuir* 17:4858–4866.

Kushwaha, S.C., M. Kates, G.D. Sprott, and I.C. Smith. 1981. Novel complex polar lipids from the methanogenic archaebacterium *Methanospirillum hungatei. Science* 211:1163–1164.

Lee, M.T., C.C. Hsueh, M.S. Freund, and G.S. Ferguson. 1998. Air oxidation of self-assembled monolayers on polycrystalline gold: The role of the gold surface. *Langmuir* 14:6419–6423.

Ligler, F.S., G.P. Anderson, P.T. Davidson, R.J. Foch, J.T. Ives, K.D. King, G. Page, D.A. Stenger, and J.P. Whelan. 1998. Remote sensing using an airborne biosensor. *Environ. Sci. Technol.* 32:2461–2466.

Ligler, F.S., T.L. Fare, E.E. Seib, J.W. Smuda, A. Singh, P. Ahl, M.E. Ayers, A.W. Dalziel, and P. Yager. 1988. Fabrication of key components of a receptor-based biosensor. *Med. Instrum.* 22:247–256.

Lingler, S., I. Rubenstein, W. Knoll, and A. Offenhausser. 1997. Fusion of small unilamellar lipid vesicles to alkanethiol and thiolipid self-assembled monolayers on gold. *Langmuir* 13:7085–7091.

Lopatin, A.N., E.N. Makhina, and C.G Nichols. 1995. The mechanism of inward rectification of potassium channels: "long-pore plugging" by cytoplasmic polyamines. *J. Gen. Physiol.* 106:923–955.

Ma, F., and R.B. Lennox. 2000. Potential-assisted deposition of alkanethiols on Au: Controlled preparation of single and mixed-component SAMs. *Langmuir* 16:6188–6190.

Meuse, C.W., S. Krueger, C.F. Majkrzak, J.A. Dura, J. Fu, J.T. Connor, and A.L. Plant. 1998a. Hybrid bilayer membranes in air and water: Infrared spectroscopy and neutron reflectivity studies. *Biophys. J.* 74:1388–1398.

Meuse, C.W., G. Niaura, M.L. Lewis, and A.L. Plant. 1998b. Assessing the molecular structure of alkanethiol monolayers in hybrid bilayer membranes with vibrational spectroscopies. *Langmuir* 14:1604–1611.

Motesharei, K., and M.R. Ghadiri. 1997. Diffusion-limited size-selective ion sensing based on SAM-supported peptide nanotubes. *J. Am. Chem. Soc.* 119:11306–11312.

Myers, V.B., and D.A. Haydon. 1972. Ion transfer across lipid membranes in the presence of gA. II. The ion selectivity. *Biochim. Biophys. Acta* 274:313–322.

Naumann, R., E.K. Schmidt, A. Jonczyk, K. Fendler, B. Kadenbach, T. Liebermann, A. Offenhausser, and W. Knoll. 1999. The peptide-tethered lipid membrane as a biomimetic system to incorporate cytochrome c oxidase in a functionally active form. *Biosens. Bioelectron.* 14:651–662.

Padeste, C., S. Kossek, H.W. Lehmann, C.R. Musil, J. Gobrecht, and L.J. Tiefenauer. 1996. Fabrication and characterization of nanostructured gold electrodes for electrochemical biosensors. *J. Electrochem. Soc.* 143:3890–3895.

Philp, D., and J.F. Stoddart. 1996. Self-assembly in natural and unnatural systems. *Angew. Chem. Int. Ed. Engl.* 35:1154–1196.

Plant, A.L. 1993. Self-assembled phospholipid/alkanethiol biomimetic bilayers on gold. *Langmuir* 9:2764–2767.

Plant, A.L. 1999. Supported hybrid bilayer membranes as rugged cell membrane mimics. *Langmuir* 15:5128–5135.

Raguse, B., V.L.B. Braach-Maksvytis, B.A. Cornell, L.G. King, P.D. Osman, R.J. Pace, and L. Wieczorek. 1998. Tethered lipid bilayer membranes: Formation and ionic reservoir characterisation. *Langmuir* 14:648–659.

Raguse, B., P.N. Culshaw, J.K. Prashar, and K. Raval. 2000. The synthesis of archaebacterial lipid analogs. *Tetrahedron Lett*. 41:2971–2974.

Ron, H., S. Matlis, and I. Rubenstein. 1998. Self-assembled monolayers on oxidized metals. 2. Gold surface oxidative pretreatment, monolayer properties, and depression formation. *Langmuir* 14:1116–1121.

Ron, H., and I. Rubenstein. 1994. Alkanethiol monolayers on preoxidized gold. Encapsulation of gold oxide under an organic monolaye. *Langmuir* 10:4566–4573.

Ron, H., and I. Rubenstein. 1998. Self-assembled monolayers on oxidized metals. 3. Alkylthiol and dialkyl disulfide assembly on gold under electrochemical conditions. *J. Am. Chem. Soc.* 120:13444–13452.

Sackmann, E. 1996. Supported membranes. Scientific and practical applications. *Science* 271:43–48.

Scheibler, L., P. Dumy, M. Boncheva, K. Leufgen, H.J. Mathieu, M. Mutter, and H. Vogel. 1999. Functional molecular thin films: Topological templates for the chemoselective ligation of antigenic peptides to self-assembled monolayers. *Angew. Chem. Int. Ed. Engl.* 38:696–699.

Schmidt, C., M. Mayer, and H. Vogel. 2000. A chip-based biosensor for the functional analysis of single ion channels. *Angew. Chem. Int. Ed. Engl.* 39:3137–3140.

Separovic, F., S. Barker, M. Delahunty, and R. Smith, R. 1999. NMR structure of C-terminally tagged gramicidin channels. *Biochim. Biophys. Acta.* 1416: 48–56.

Steinem, C., A. Janshoff, W.P. Ulrich, M. Sieber, and H.J. Galla. 1996. Impedance analysis of supported lipid bilayer membranes: A scrutiny of different preparation techniques. *Biochim. Biophys. Acta* 1279:169–180.

Stelzle, M., G. Weissmuller, and E. Sackmann. 1993. On the application of supported bilayers as receptive layers for biosensors with electrical detection. *J. Phys. Chem.* 97:2974–2981.

Stetter, K.O. 1996. Hyperthermophilic prokaryotes. *FEMS Microbiol. Revs.* 18:149–158.

Stora, T., J. Lakey, and H. Vogel. 1999. Ion-channel gating in transmembrane receptor proteins: Functional activity in tethered lipid membranes. *Angew. Chem. Int. Ed. Engl.* 38:389–392.

Suarez, E., E.D. Emmanuelle, G. Molle, R. Lazaro, and P. Viallefont. 1998. Synthesis and characterization of a new biotinylated gramicidin. *J. Peptide Sci.* 4:371–377.

Terrettaz, S., H. Vogel, and M. Grätzel. 1998. Determination of the surface concentration of crown ethers in supported lipid membranes by capacitance measurements. *Langmuir* 14:2573–2576.

Toro-Goyco, E., A. Rodriguez, and J. del Castillo. 1966. Detection of antiinsulin antibodies with a new electrical technique: Lipid membrane conductometry. *Biochem. Biophys. Res. Comm.* 23:341–346.

Tsai, M.Y., and J.C. Lin. 2001. Preconditioning gold substrates influences organothiol self-assembled monolayer (SAM) formation. *J. Colloid Interface Sci.* 238:259–266.

Ufheil, J., F.M. Boldt, M. Börsch, K. Borgwarth, and J. Heinze. 2000. Microstructuring of solid-supported lipid layers using sam pattern generation by scanning electrochemical microscopy (SECM) and the chemical lens. *Bioelectrochemistry* 52:103–107.

Ulman, A. 1996. Formation and structure of self-assembled monolayers. *Chem. Rev.* 96:1533–1554.

Walczak, M.M., C.A. Alves, B.D. Lamp, and M.D. Porter. 1995. Electrochemical and X-ray photoelectron spectroscopic evidence for differences in the binding sites of alkanethiolate monolayers chemisorbed at gold. *J. Electroanal. Chem.* 396:103–114.

Wallace, B.A. 1998. Recent advances in the high resolution structures of bacterial channels: Gramicidin A. *J. Struct. Biol.* 121:123–141.

Woodhouse, G., L. King, L.Wieczorek, P. Osman, and B. Cornell. 1999. The ion channel switch biosensor. *J. Mol. Recogn.* 12:328–335.

Yager, P. 1988. Development of membrane-based biosensors: Measurement of current from photocycling bacteriorhodopsin on patch clamp electrodes. *Adv. Exp. Med. Biol*. 238:257–267.

Zaitsev, S.Yu., S.V. Dzekhitser, and V.P. Zubov. 1988. Polymer monolayers with immobilized bacteriorhodopsin. *Bioorg. Khim.* 14:850–852.